

Three-Dimensional Flow Visualization for the Steady and Pulsatile Flows in a Branching Model using the High-Resolution PIV System

Sang-Ho Suh¹ and Hyung Woon Roh

Department of Mechanical Engineering, Soongsil University

Abstract

The objective of the present study is to visualize the steady and pulsatile flow fields in a branching model by using a high-resolution PIV system. A bifurcated flow system was built for the experiments in the steady and pulsatile flows. Harvard pulsatile pump was used to generate the pulsatile velocity waveforms. Conifer powder as the tracing particles was added to water to visualize the flow fields. CCD cameras (1K×1K(high resolution camera) and 640×480(low resolution camera)) captured two consecutive particle images at once for the image processing of several cross sections on the flow system. The range validation method and the area interpolation method were used to obtain the final velocity vectors with high accuracy. The results of the image processing clearly showed the recirculation zones and the formation of the paired secondary flows from the distal to the apex of the branch flow in the bifurcated model. The results also indicated that the particle velocities at the inner wall moved faster than the velocities at the outer wall due to the inertial force effects and the helical motions generated in the branch flows as the flow proceeded toward the outer wall. Even though the PIV images from the high resolution camera were closer to the simulation results than the images from the low resolution camera at some locations, both results of the PIV experiments from the two cameras generally agreed quite well with the results from the computer simulations. Therefore, instead of using the expensive stereoscopic PIV or 3D PIV system, the three-dimensional flow fields in a bifurcated model could be easily and exactly investigated by this study.

Key words: Blood Flow Characteristics, Three-Dimensional Flow Visualization, Pulsatile Flows, PIV System

Introduction

A circulatory system where it transfers blood or industry fluids consists of not only straight tubes but also curved tubes including different diameters in size or the bifurcated angles. Also, the flow phenomena in the human vessels or in the industrial pipes show a periodic pulsation flow due to the movements of the heart or the pump. Blood in the curved artery or in the bifurcated artery usually do not flow smoothly, and the blockage phenomena in the blood vessels can be easily happened. These blockage phenomena cause atherosclerosis in the blood vessels (Banerjee, 1992) or a scale in the industrial fields. There are several hypotheses for the occurrence of the atherosclerosis in the human vessels. Among the many hypotheses, the repeated wall shear stresses model (fatigue stress or repeated stress) due to

the generations of the helical flow or the separated flow in the curved or the bifurcated arteries is the most well known hypothesis.

In order to closely understand the blockage phenomena, the three-dimensional pulsatile flow in the bifurcated duct must be investigated (Huges and How, 1995). Many researchers have been investigated to obtain the three-dimensional flow fields using the stereoscopic PIV, 3-D PIV, or the numerical method. However, most of the studies in the three-dimensional flow fields were based on the numerical methods rather than based on the experimental measurements due to the several difficulties and restrictions on those experimental setups. Thus, this study investigated the three dimensional pulsatile flow characteristics in the bifurcated duct using a high-resolution PIV system instead of using the expensive stereoscopic PIV or 3-D

¹ 1-1 Sangdo-dong Dongjak-gu, Seoul, 156-743, Korea
E-mail: suhsangho@rocketmail.com

PIV system, and the results from the measurements were compared with those from the numerical simulations.

PIV experiment

The schematic diagram of the experimental setup is shown in Fig. 1. The PIV system is composed of fiber optic, AOM, CCD camera, and a light source with the 5W argon-ion laser sheet beam. The focus lens was used to prevent the laser source beam from scattering and to increase the beam intensity. A point light source through the fiber optic was changed to the sheet beam across the right surface area of the rectangular channel (20×20mm). The CCD cameras (1K×1K(high resolution camera) and 640×480(low resolution camera)) were used to detect the scattering light. In order to obtain images from the flow visualization experiment using the PIV, the tracer or tracking particles with almost the same physical properties as the working fluid should be added into the flow field. For the flow visualization, conifer powder, whose homogeneous particles has a diameter of about 50 μm, was used as the tracer particles on the basis of the results from the prior research (Suh. et al., 1999). In order to investigate the three-dimensional flow phenomena, continuous raw images were acquired with very short time interval in the several sections from the centerline in 3 mm intervals (see Fig. 2). Havard pulsatile pump was used to generate the pulsatile velocity waveforms (Roh, 1999). Displacement volume of the pulsatile pump was designed to control the systole and diastole ratio, and its maximum capacity was 100 ml

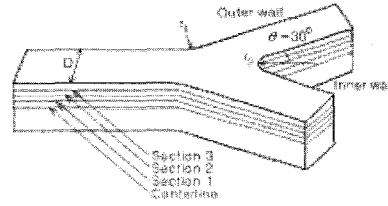


Figure 2 Geometric configuration of the branching model

For the image processing in the PIV, the two-frame cross-correlation method is widely used to obtain velocity vectors. The cross-correlation coefficients are calculated by comparison with the gray level concentrations of two correlation areas in two consecutive images. Given infinitesimal intervals of time, the two-frame method among the various image-processing techniques is employed to examine two consecutive images acquired for the duration of the predetermined time steps. The velocity for image processing from the binary images in both traced particle and background image is calculated by computing the displacement of the particles to be moved during the infinitesimal interval of time. In such a way, the gray level cross correlation method is incorporated into the flow velocity acquisition.

Computer Simulation

In order to investigate the pulsatile flow characteristics in the bifurcated duct, the following continuity and momentum equations are used for the computer simulation.

$$\frac{\partial u_j}{\partial x_j} = 0 \tag{1}$$

$$\rho \left(\frac{\partial u_i}{\partial t} + u_j \frac{\partial u_i}{\partial x_j} \right) = - \frac{\partial p}{\partial x_i} + \eta \frac{\partial}{\partial x_j} \left(\frac{\partial u_i}{\partial x_j} + \frac{\partial u_j}{\partial x_i} \right) \tag{2}$$

where ρ, u_i, p, and η are density, velocity vector, pressure, and apparent viscosity, respectively. The geometric shape of the bifurcation model used in the computer simulation is the same as the one used in the experiment. Water, the Newtonian fluid, is applied, and the inlet condition is a fully developed flow of 400 in the Reynolds number. The governing equations for the pulsatile flow are discretized by the finite volume method.

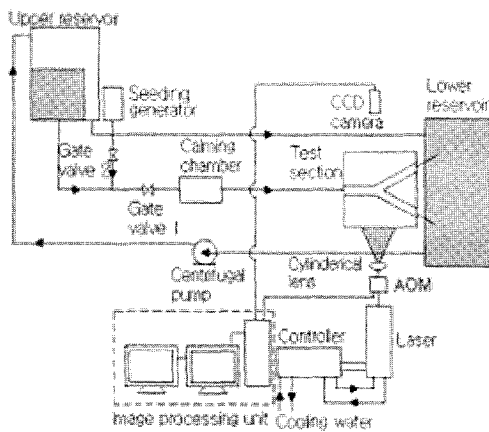


Figure 1. Schematic diagram of the experimental setup with the PIV system

The upwind differencing scheme is adapted for discretization of the convective terms and the SIMPLE-C algorithm for treating the pressure terms in the momentum equations. The pressure boundary condition is imposed on the outlet boundary condition, and the convergence criteria is 1×10^{-7} of the relative error to the flow velocity. Grid numbers used in the calculation are $10 \times 10 \times 105$.

Results and Discussion

Steady flow

Due to the helical flows generated downstream to the outer walls after the bifurcation apex, it was difficult to acquire the velocity vectors. Thus, the PIV experiments using high resolution high-resolution camera were conducted at the steady flow for $Re=400$ as we can see from Fig. 3 and Fig. 4. Those figures also show the results of the PIV experiments using low resolution camera. In order to accurately investigate the steady flow phenomena in the three-dimensional flow of the bifurcated duct, the computer simulations besides the experimental measurements were conducted with the same geometrical and physical conditions. To assure the validation of the velocity vectors obtained by the PIV, the dimensionless velocity profiles in several cross sections of the trunk were compared with the results from the simulation as can be seen in Fig. 3.

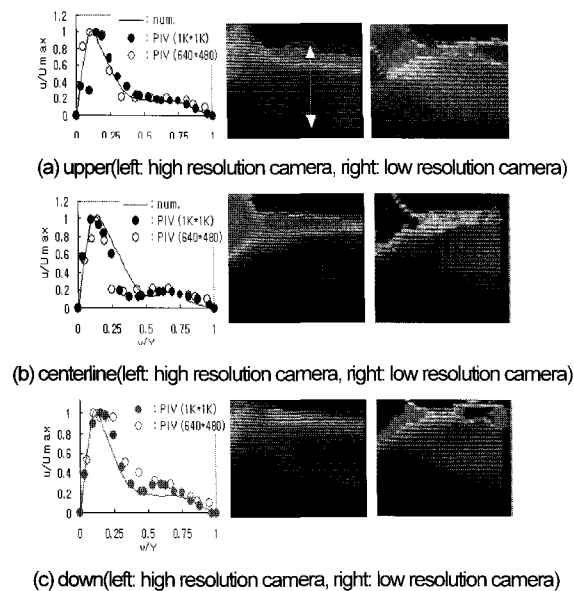


Figure 3. Comparison of the velocity profiles obtained by the PIV experiment and computer simulation

The results obtained from the PIV experiments and the computer simulation showed that the branch flow

strongly pushed the flow particles into the inner wall due to the inertial effects, and accompanied helical motions as it moved toward the outer walls. The results also showed the recirculation zones and the formations of the paired secondary flow from the distal to the apex of the bifurcation model. The PIV results of the high resolution camera showed similar tendency with the results of the low resolution camera. However, erroneous velocity vectors from the low resolution camera case were appeared near the inner wall at the distal region of bifurcated duct due to the camera's rough spatial resolution.

Fig. 3 (a) and 3 (c) are the upper and the down sections of the centerline in 3 mm interval and Fig. 3 (b) is the velocity profiles in the centerline of the bifurcated trunk, respectively. As you can see from Figs. 3(a), (b) and (c), radial velocity distributions near the inner wall were larger and dense due to the strong particle movements into the inner wall (also can be seen from Fig. 4). The formations of the recirculation near the outer wall were smaller than those near the inner wall. This tendency of the velocity distribution in the centerline plane could be found in the velocity distributions in the upper and down planes (see Figs. 3 (a) and 3 (c)).

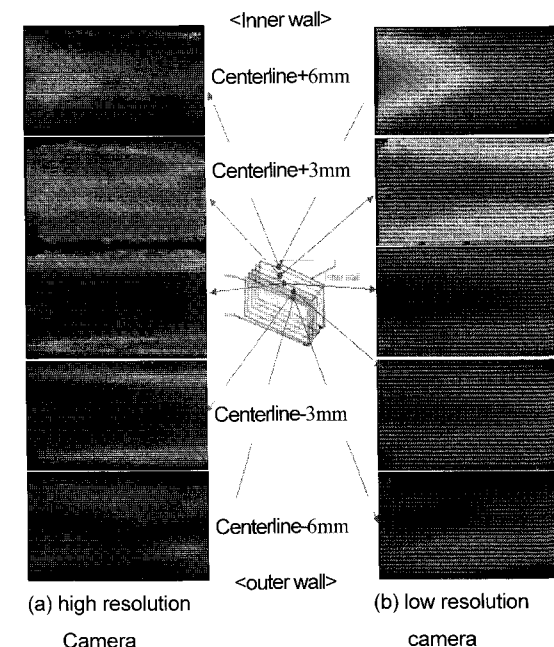


Figure 4. Comparison of the results of the PIV experiment

Whole magnitude of velocity distributions near the outer wall in the centerline plane were smaller and came to be flat than those of velocity distributions on another

places in the centerline plane due to the secondary flow effects. The results from both of the computer simulations and the PIV experiments were agreed quite well each other. While comparing the results from Fig. 3 with the results from Fig. 4, it was found that PIV experiments using the high resolution camera were closer to the numerical simulations than the PIV experiments using the low resolution camera. However, even though PIV images from the high resolution camera were closer to the numerical simulation results than the images from the low resolution camera at some locations, both results of the PIV experiments from the two cameras generally agreed well each other.

The velocity maps of the several vertical planes in the bifurcated trunk are shown in Fig. 4. The planes of “centerline+6mm” is near to the inner wall and the plane of “centerline-6mm” is near to the outer wall of the bifurcated trunk. Velocity maps of the “centerline+6mm” plane near the inner wall had more strong flow fields due to the inertial force than those of the “centerline-6mm” plane. The strong velocity vectors in top and bottom regions of the centerline plane were to be caused by the secondary flow formed from the bifurcated effects and the inertial forces. As you can see from Fig. 4, the obtained velocity maps by high resolution camera were analogous to the velocity maps by low resolution camera. Therefore, instead of using the expensive stereoscopic PIV or 3D PIV system, the three-dimensional flow fields in steady state could be easily and exactly investigated using the 2D CCD cameras.

Pulsatile flow

In order to investigate the characteristics in a three-dimensional pulsatile flow, the PIV experiments using the high resolution camera, low resolution camera, and numerical simulation were conducted. Harvard pulsatile pump was installed to make the pulsatile flow at the inlet region of the bifurcated duct (capacity: 30liter/sec, ratio of systole and diastole: 50:50, period: 1.1sec). Due to the generations of the secondary flow and the helical flow, previous study (Suh et al., 1999) described that the phenomena of the pulsatile flow were much more complex than those of the steady flow.

Particle-tracking method were adapted to closely investigate the pulsatile flow for the bifurcated duct using the computer simulations at each time step as can

be seen from Fig. 5. The used time step and the period were 1/30 s and 1.1 s, respectively. Figures 5 (a) and 5 (b) are the results of the particle trajectories at the first acceleration phase and at the maximum velocity phase, respectively. Figures 5 (c) to 5 (f) are the results of the particle trajectories at the deceleration phase.

During the acceleration phase, no recirculation zone was observed in the flow field, and the velocity vectors were appeared in an orderly fashion for all over the flow field (see Figs. 5 (a) and 5 (b)). However, for the deceleration phase ((Figs. 5 (d), 5 (e), and 5 (f)), the velocity vectors at the inner wall of the daughter branch were inwardly skewed due to the centrifugal force, and the recirculation zones were built up at the outer wall of the bifurcated duct. As we can see from Fig. 5 the particle tracking method could fully express the three-dimensional flow characteristics in the bifurcated duct.

Many researchers have been investigated to obtain the three-dimensional flow field using the stereoscopic PIV, 3-D PIV, and etc. However, since the principle of the PIV method is to obtain the 2D velocity map using the captured raw images in 2D plane, it was difficult to obtain the three-dimensional velocity maps using those conventional methods. This study analyzed the three dimensional pulsatile flow characteristics from the measured raw image maps in several planes at the specified times (acceleration phase and deceleration phase) as can be seen from Fig. 6.

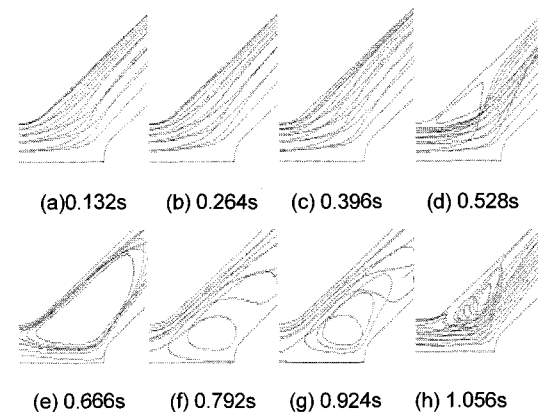


Figure 5 Pictures showing particle path during the cycle of pulsatile flow

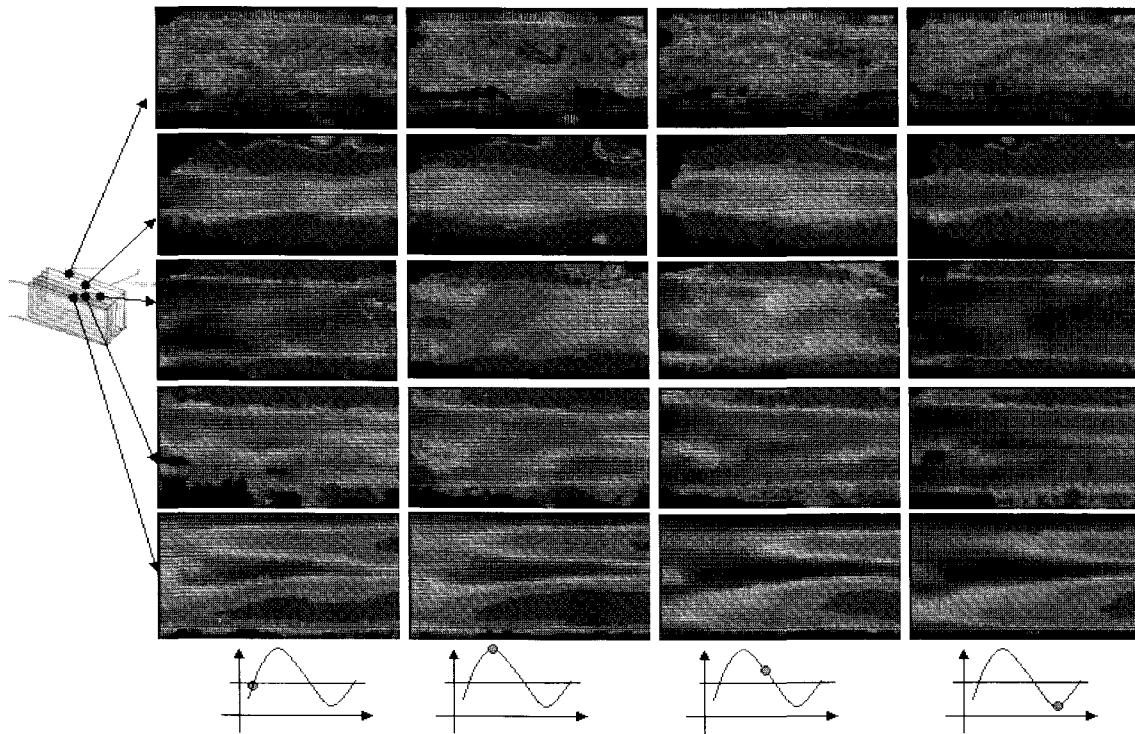


Figure 6. Obtained velocity maps during the cycle of pulsatile flow using high resolution camera

Velocity maps in the several sections from the centerline (3 mm intervals) are shown in Fig. 6 during the whole one cycle. For the acceleration phase, the branch flow was moved strongly into the inner wall due to the inertial force effects. However, for the deceleration phase, helical motions were generated as the flow proceeded toward the outer wall. These tendencies are an important phenomenon to understand the etiology and pathogenesis of diseases in the field of hemodynamics since the regions of high shear stress could be localized along the inner wall. The three-dimensional flow fields in the pulsatile flow could be successfully investigated by this study instead of using the expensive stereoscopic PIV or 3D PIV system.

Conclusions

The characteristics of the three-dimensional pulsatile flow in the section of bifurcated duct were successfully investigated, and the results from the PIV experiments were agreed well with the results from the numerical simulation (see Figs 5 and 6). For the acceleration phase, the pulsatile flow in the bifurcated duct was moved strongly toward the inner wall due to the inertial force effects. However, for the deceleration phase, helical

motions were generated as the flow proceeded toward the outer wall. These trends could be also found in the results from the numerical simulation. Both of the results from the PIV experiments and the numerical simulation also showed the recirculation zones and the formation of the paired secondary flows at the locations from the distal to the apex of the bifurcated duct. While the PIV images from the high resolution camera were closer to the simulation results than the images from the low resolution camera at some locations, both results of the PIV experiments from the two cameras generally agreed quite well with the results from the numerical simulation. Therefore, instead of using the expensive stereoscopic PIV or 3D PIV system, the three-dimensional flow fields in a bifurcated duct could be easily and accurately investigated by this study.

Acknowledgement

This work was supported by grant No. R01-2002-000-00561-0(2002) from Basic Research Program of the Korea Science & Engineering Foundation

References

1. Adrian RJ. Particle-Imaging Techniques for Fluid Mechanics. *Ann. Rev. Fluid Mech.*, 1991;23:261-304.
2. Augi J. and Jimenez J. On the performance of particle tracking. *J. Fluid Mech.* 1987;185:447.
3. Banerjee, RK. A Study of Pulsatile Flows with Non-Newtonian Viscosity of Blood in Large Arteries. Ph.D. Thesis, Drexel University, 1992.
4. DH Doh, SH Choi, TS Baek, and YW Lee, T. Kobayashi and T. Saga. Measurement of 3-Dimensional Velocity and Pressure Distribution of a Complex Flow by 3-D PTV, *Proc. of 4th KSME-JSM EFluids Eng. Conf.*, 1998;365-368.
5. Hughes PE and How TV. Flow Structure at the Proximal Side-to-End Anastomosis. Influence of Geometry and Flow Division, *Journal of Biomechanical Engineering*, 1995;117:224-236.
6. Lee YH, Cho DH and Seo MS. A PIV Analysis of Confined Jet Mixing Flow within Circular Pipe, *JSME Centennial Grand Congress International Conference on Fluid Engineering*, 1997;663-668.
7. Roh HW. Pulsatile Flow Analysis of Non-Newtonian Fluids in the Circular and Bifurcated Tubes, Ph. D. Thesis, Soongsil Univ., 1999.
8. Suh SH, Roh HW, Cho MT and Yoo SS, Visualization of Unsteady Flow of Newtonian and Non-Newtonian Fluids in the Circular and Bifurcated Tubes, '99 Korea-Japan PIV Joint Seminar, 1999;68-77.